BNL 10565
CONF-660918-2
CFSTI PRICES

H.C. $ 2.00 MN .50

RADIOFREQUENCY BEAM SEPARATOR AT BROOKHAVEN*

H. Hahn

Brookhaven National Laboratory, Upton, New York

(Invited paper to be presented at the 1966 International Conference on Instrumentation for High Energy Physics at Stanford, California).

*Work performed under the auspices of the U.S. Atomic Energy Commission.

DISCLAIMER

I. INTRODUCTION

The Brookhaven radiofrequency beam separator was installed, together with a beam transport system, in the North Area of the Alternating-Gradient Synchrotron during the scheduled AGS shutdown in November 1965. After a short period of debugging and testing, the operation of the rf beam for the physics research program began in January 1966. The design studies for this type of separator, which is based on a proposal made by Panofsky in 1959 and detailed by a group at CERN, started at the Brookhaven National Laboratory and Yale University in 1961. The construction of the apparatus, which took roughly three years, was carried out by the Accelerator Department of BNL. In this context it has to be mentioned that the first rf separator of this type, which produced 10 GeV/c kaon beams, was put into operation at the CERN Proton Synchrotron early in 1965.

The start-up of the separated beam was somewhat retarded by difficulties with the fast beam extraction system and by problems resulting from misalignments of the magnets; the rf separator proper went into operation without significant modifications. From the experience gained during several runs, one can conclude that the operation of the rf separator is simpler and generally more reliable than electrostatic separators. As of today, exposures for the experiments listed in Table I have been completed. A failure of the 80-inch bubble chamber interrupted the operation and prevented this list from being considerably longer. Beam No. 4 with switched-off deflectors can also serve as transport system for unseparated π^- and p beams up to 30 GeV/c and it was used for pp exposures at 29 GeV/c and π^-p exposures at 16 and 25 GeV/c.

The pulsed operation of the rf separator and the desire to achieve high particle fluxes by using 0^{o} production angles imposes the use of a fast external beam. Typically, two of the 12 circulating bunches are extracted, which results in about 2×10^{11} extracted protons of about 25 GeV per machine pulse. Recently, one bunch extraction was made feasible. As a consequence, a highly desirable parasitic operation of the rf separated beam is standard.

Previous to the installation of the rf separated beam, the bubble chamber was served by HESB No. 3, a two-stage electrostatically separated beam with a maximum momentum of about 8.5 GeV/c. When operated at 500 kV across the 10 cm gap, the two ES separators, each 15 m long, are capable of providing, for instance, kaon beams of up to 5.5 GeV/c. At present, a rebuilt version of the dc beam and the rf beam are coexistent (Fig. 1). This was made possible by using an internal target for the dc beam and an external target for the rf beam, and by making a provision for moving the bubble chamber to either beam line. The regions of operation of the two beams are complementary; together they cover practically the entire high energy range of interest at the AGS.

The principle of the rf beam separator to be discussed may be outlined as follows: The unbunched beam of secondary particles, i.e., a beam without microwave structure, is momentum analyzed and then imaged into a first "point" deflector where wanted (W) and unwanted (U) particles receive the same time harmonic vertical deflection, $\hat{\theta} \exp(j\omega t)$. The particle beam is reimaged into a second deflector, separated from the first by a drift length, L . W and U particles have different rest masses, m_W and m_U , and different velocities, v_W and v_U . They will, therefore, arrive at the

second deflector with a phase difference relative to the circular frequency, ω , in the deflectors of $\tau = \omega L \{ v_W^{-1} - v_U^{-1} \}$, which becomes, in relativistic approximation, $\tau \approx \frac{1}{2} \omega L (m_W^2 - m_U^2) / p^2$. The second deflector produces the same time harmonic deflection as the first one. For a certain combination of frequency, length and momentum, the phase slip between particles will equal π . In this case, it is possible to arrange the relative phase of both deflectors so that cancellation of deflections occurs for U particles, whereas the time harmonic deflection of the W particles is doubled. W particles are fanned out after their emergence from the second deflector and will, at least in part, pass the so-called beam stopper which, on the other hand, degrades all of the U particles. A pure beam of W particles will enter the bubble chamber after a post-momentum analysis.

The advantages of the rf separation principle in comparison to dc separators should be obvious. In both separators use is made of the fact that W and U particles receive a different transverse momentum, p_T , when passing through the separation stage. In ES separators the usable transverse momentum equals the difference in deflections which in turn is determined by the difference in time of flight, i.e., $p_T \propto E_{dc} \ell (m_W^2 - m_U^2) / p^2$. In rf separators the difference in time of flight defines only which kind of particle will receive a deflection and the usable peak transverse momentum itself equals twice the full deflection, i.e., $p_T \propto E_{rf} \ell$ and the p^{-2} factor no longer enters. An additional, although minor advantage, lies in the fact that the effective electric field attainable in rf deflectors during short pulses can exceed the dc breakdown field strength. As a result of the difficulties mentioned, ES separators have an upper momentum limit, whereas

properly designed rf separators are likely to remain feasible at momenta well above 100 GeV/c. On the other hand, rf separators are limited towards lower momenta because of chromatic phase errors inherent to the rf separation scheme or because of difficulties with the inter-deflector beam optics, if the drift space between deflectors is reduced. Moreover, the rf separators built so far are limited to bubble chamber work due to the mandatory pulsed operation. Further disadvantages of a simple two-deflector rf separator with fixed drift length are its limitation to certain selected momenta and the unavoidable losses of from 50 to 80 percent of W particles in the beam stopper. However, these drawbacks are not of fundamental nature, since the development of superconducting cavities would allow cw operation and the addition of a third deflector or the use of circularly polarized deflectors could result in operation over a wide range of momentum.

II. PARAMETERS OF RF SEPARATOR

The basic choice in designing an rf separator is the operating frequency, which, ideally, is selected to provide maximum transmission of W particles. The drift space, L, between deflectors is prescribed by the particle kinematics. At a given operating momentum, $L \propto \lambda$. To avoid excessive decay of unstable particles the deflector distance should be kept at a minimum, favoring a high frequency. On the other hand, the total acceptance increases with λ and lower frequencies are preferable. Practical frequency ranges are L, S and X band (1 to 10 GHz). For the rf beam separator at the AGS, L band was excluded by the limited space between synchrotron and bubble chamber. The lack of adequate amplifiers at X band dictated the choice of the standard linac frequency in S band, at which high power klystrons and other equipment are readily available. For the BNL separator, $\lambda_o = 10.5$ cm and $L = 40$ m were chosen, whence follows the design momentum $p_o = 9.25$ GeV/c for $K\pi$ separation.

The total beam length between external target at the AGS straight section I-13 and the 80-inch bubble chamber is about 129 m. The beam optics in the separated version may be divided functionally into three sections: (1) pre-momentum analysis section, (2) separation stage from source slit, C3, to beam stopper, C5, and (3) post-momentum analysis section. It will not be attempted here to present a discussion of the beam optics, nevertheless a summary of the principal optical parameters is given in Table II. Some comments are, however, thought to be helpful in this context. The momentum analysis is performed in the horizontal plane, whereas the separation of particles occurs in the vertical plane. The permissible momentum bite of the beam is restricted by chromatic aberrations of the separator and the problem of muon background to a value smaller than 1%. The separation stage proper consists of the recombination section, the interdeflector section, and the stopper section. The recombination section exactly cancels the momentum dispersion introduced for the pre-momentum analysis. The source slit, located at the vertical object focal plane of the recombination section, defines the vertical angular divergence of the beam in the deflectors and represents the effective source of the separation stage. The quadruplet of the interdeflector section images the first deflector into the second deflector with unit magnification in both planes. In addition, this section insures that the vertical phase space of the beam in the first deflector is reproduced in the second deflector, allowing perfect cancellation of displacements as well as angular deflections of U particles. In the stopper section differences in angular deflections are converted into differences of position. Consequently, it is possible that U particles strike the beam stopper and lose energy, whereas W particles

continue their flight to the bubble chamber unaltered. The post-momentum analysis which follows then permits a complete physical separation of W and U particles.

An important characteristic of a beam transport system is its acceptance. Although the acceptance of the Brookhaven rf separator is limited by the magnetic optics, it is instructive to evaluate the intrinsic acceptance of the deflectors alone. The maximum useful acceptance of the rf separator is calculated under the assumption that the aperture of the deflector is limited by the inscribed square. The optimum filling is achieved if, for the deflector with radius a and length ℓ, the horizontal and vertical beam phase space are $\Delta_H = a^2/\ell$ and $\Delta_V = \frac{1}{3} a^2/\ell$, respectively. The factor 1/3 is to accommodate the phase space occupied by the vertically deflected particles. The Brookhaven deflector has $a \approx 2.4$ cm and $\ell \approx 3.3$ m when cut-off tubes at each end are included. It follows that the total acceptance $\Delta = \Delta_H \Delta_V \approx 100$ cm^2 μsterad. The various collimators which are necessary to provide a well-defined aperture for the beam reduce the total acceptance considerably. However, the loss in acceptance entails in the case of the Brookhaven separator no serious disadvantage since, with the possible exception of antiprotons, no flux limitation was encountered.

The principle of the rf separator was explained for the case of a two-component beam in which one contaminant is to be removed. Actually, the conditions are somewhat different. Proton and π^- beams are possible without separation. π^+ require the removal of protons and the rf separator functions as discussed. K^- and $\bar{p}$ beams require a two-contaminant rejection, and in K^+ beams the rejection of three contaminants, p, π^+, d, is necessary. It turns out that operation of the rf separator with two-contaminant rejection

is possible at certain selected momenta only, whereas a one-contaminant rejection is feasible in comparatively large momentum bands. The condition for a two-contaminant rejection is established by the requirement that the phase shift between the two kinds of U particles at the second deflector equals a multiple of 2π, $\tau_{U1} - \tau_{U2} = 2\pi \times m$, with m being an integer. If this condition is established it becomes, obviously, possible to adjust the phase between deflectors such that the deflections of both U particles cancel exactly. However, the deflection of W particles is in this case not necessarily maximum and it is convenient to express the achievable deflection by way of the "deflection efficiency", ϵ_W, which is defined as the ratio of actual deflection to maximum deflection. As illustration, the operating momenta of K beams and relevant quantities are listed in Table III. ϵ_K and ϵ_d are the deflection efficiencies of kaons and deuterons. Note that ϵ_d' includes the reduction in deflection due to the asynchronism of the deuterons in the deflector. The deflection efficiency of the predominant contaminants, pions and protons, is represented by ϵ_U. It is seen that a tight pre-momentum analysis is necessary to avoid achromatic aberrations in the separator stage. Moreover, operation with $m > 3$ is undesirable for the same reason. As a general rule, errors of any kind will result in a finite residual deflection of U particles. This will cause a reduced purity of the beam, or a reduction in flux of W particles, if the beam stopper size is increased to compensate for the residual deflections.

Source slit and beam stopper size are fully adjustable and their optimal settings for high purity and maximum flux have to be found empirically for each experiment. A typical source slit opening is 1.4 cm, which results in a total angular divergence of the beam at the deflectors of about 0.6 mrad.

The rf power fed to the deflectors is adjusted to produce about ϵ_W^{-1} mrad peak deflection in a single deflector, resulting in a total deflection of 2 mrad for the W particles. The beam stopper size is normally larger by a factor 3 to 4 than the undeflected image width which would correspond to the source slit setting. Losses of W particles in the beam stopper lie, therefore, in the 50 to 80% range.

The increase in beam stopper size is necessary to intercept U particles with finite residual deflections which may be caused by anisochronism of off-momentum particles or by amplitude and phase errors of the rf field in either deflector. In addition, the increased beam stopper size allows for a degradation of beam-like, i.e., on-momentum, muons produced by pion decay in flight. In fact, this is probably the most exacting requirement in K beams. Non-beam-like muons will be prevented from entering the bubble chamber by the post-momentum analysis. Beam-like muons originating before the momentum slit, C3, behave like pions, and are focused on the beam stopper. Beam-like muons originating in the separation stage have a well-defined decay angle, ζ , and the minimum beam stopper is therefore determined as the angular divergence of the beam plus twice the decay angle ζ . The decay angle for beam-like muons is approximately given by $\zeta \approx 12.5\ p^{-1}$ mrad GeV/c for muons with 2% variation from nominal momentum. Contaminants produced by kaon decay after the magnetic slit, C6, cannot be removed from the beam and represent the ultimate limitation in beam purity. Incidentally, scanning results from a K^+ run at 7.4 GeV/c are consistent with this limit value (6% background).

III. DEFLECTOR

Proper operation of the rf beam separator requires deflectors which are capable of imparting a transverse momentum $p_T \geq 18$ MeV/c to traversing particles when powered from available klystrons. Moreover, it is desirable that the deflections be aberration free. An iris-loaded waveguide operating in the lowest hybrid mode with dipole character was, therefore, chosen as deflecting structure. The design of the deflector had to be finalized at a time when the properties of this type of structure were mostly unknown, and the solution adopted is not necessarily optimum.

The design of the BNL deflector proceeded along the following line. The operating wavelength was imposed by considerations elaborated above to be 10.5 cm. Traveling wave operation was preferred because of the smaller breakdown problems and the possibility of changing the phase velocity. The number of irises per wavelength, N = 4, resulted from a compromise between acceptance (greater for high N) and shunt impedance (greater for low N). A conventional value of about 5 mm for the iris thickness was taken and the iris edges are rounded by machining to reduce the danger of electrical breakdown. The transverse momentum imparted by a structure which is optimized for an attenuation parameter, $\alpha \ell \approx 1.256$, is given by $p_T c \approx 0.9 q (R P \ell)^{\frac{1}{2}}$. Assuming that the available klystron power P = 15 MW and the shunt impedance R = 10 MΩ/m , it follows that the deflector length is at least 3 m. The optimum attenuation parameter is obtained by a correct choice of the group velocity, $v_g/c = \frac{1}{2} k \ell/Q \alpha \ell$, whence $v_g/c \approx 0.01$ for Q = 8000. Mechanical tolerances and electrical breakdown problems are alleviated by a larger value of the group velocity, say $v_g/c = 0.02$. The desired group velocity can be achieved in the deflecting mode with three

different openings of the beam hole, the smallest yielding the highest shunt impedance. A medium value of the beam hole represents a reasonable compromise between acceptance and shunt impedance and avoids the degeneracy encountered with the large openings. Rotation of the dipole mode was prevented by means of lateral mode stabilizing rods, which are well suited to the brazing technique employed for the fabrication of the deflectors.

The geometrical dimensions and the more important characteristics of the final BNL deflectors are listed in Table IV. The deflector constant quoted as $K\,\ell = 5.22\ k\Omega^{\frac{1}{2}}$ was obtained in deflection tests performed on the deflectors after their installation in the beam line. The result corresponds to a shunt impedance of 13.8 MΩ/m. Using this value, it can be concluded that a peak power of about 12 MW suffices to provide the required transverse momentum. The deflectors were tested at 18 MW levels without excessive arcing, insuring a comfortable safety margin in deflection.

It is desirable that the operating frequency be variable so as to make the propagating wave exactly synchronous with the W particles. The U particles will then fall out of step by $\psi = \frac{1}{2}\, k\, \ell\, (m_U^2 - m_W^2) / p^2$ and their deflection will be reduced to $2\, \psi^{-1} \sin \frac{1}{2}\, \psi$. This reduction is highly desirable. In fact, it is the only reason why deuteron contamination of K^+ beams can be avoided. Synchronism between W particles and the deflecting wave has the added advantage that a deflector of finite length behaves just like the point deflector which was assumed for the description of the separator principle. Incidentally, a change in frequency is essential for the anticipated deuteron beams which will use the deflectors as Blewett-type separators. Rf separators of this type make use of the phase slip between particles within the deflector, rather than over a drift

length. The requirement for synchronism imposes a frequency stability of about 10^{-5}, which is easily attained. However, the phase requirements between deflectors require a frequency stability of 10^{-6} and temperature changes in the deflector of less than $\pm 0.1^{\circ}C$.

The deflector is sealed off at the rf couplers by ceramic windows and it is pumped through cut-off pipes which are provided for the passage of the particle beam. Two 200 ℓ/sec sputter-ion pumps on each end hold the deflector vacuum at about 10^{-7} torr. The deflector vacuum is separated from the vacuum in the beam guide by 6 μm Mylar windows. In case of a pressure increase in the beam guide, the deflectors are automatically valved off. An rf window on the deflector input separates the deflector and waveguide vacuum system although it is not absolutely necessary. However, it allows for an easy removal of the klystron and, moreover, it was found that it acts as protection for the klystron window in case of deflector arcing.

IV. MICROWAVE SYSTEM

The purpose of the microwave system is the generation of rf pulses in both deflectors at the correct frequency (about 2856 MHz), amplitude (up to 15 MW), duration (4.5 μsec flat-top) and phase. The attainable purity of the separated beam depends largely on how well the deflections of U particles can be made to cancel. Since a major cause for residual deflections of strongly interacting particles are phase and amplitude errors of the deflections, it is understandable that the design of the microwave system aimed primarily at achieving a high stability. The required tolerances depend, of course, on the settings of source slit and beam stopper, but in order to avoid undue losses of W particles in the

beam stopper, it was specified that the phase error between deflectors should not exceed 10^{o} and that the difference between deflections remain below 6% peak-to-peak during the 2.7 μsec corresponding to a single turn ejected AGS beam pulse. Since actually only two bunches are extracted, the beam pulse length is reduced to about 0.3 μsec and the apparent stability of the microwave system is increased correspondingly.

The block diagram of the microwave system adopted for the BNL deflector is shown in Fig. 2. Although it will not be attempted to present the underlying design considerations, it is thought necessary to discuss the more interesting aspects of this approach. The common frequency source, located in the central control station, consists of a klystron oscillator which is phase-locked to a quartz reference. The rf signal is amplified to a 10 W level by means of a traveling wave tube. The output power is split in a 3 dB coupler and each signal is transmitted to one of the deflector stations via semiflexible air-dielectric coax cables. Even though the cable selected is built for a low temperature coefficient, it was held necessary to provide a phase servo system, which keeps the phase difference between cable ends at the preset value. At the deflector station the cable feeds into a plate-pulsed triode amplifier. Unless pulsed, the input of the triode amplifier acts like a short circuit and reflects the drive signal. The reflected signals are channelled through four-port circulators to a phase bridge, where the phase difference between cable ends is directly measured and a dc error signal is produced. The error signal acts on a motor-driven phase shifter in series with one of the cables and provides necessary corrections of the cable length. The triode amplifier serves directly as driver stage for the high power klystron. The klystron which was developed for SLAC

meets all requirements of the rf separator and the permanent magnet focused version built by RCA is used. The high power from the klystron is fed to the deflectors through evacuated heavy wall waveguide with inner dimensions corresponding to WR - 284. The klystron cathode pulse is produced by a line type modulator which relies on a hydrogen thyratron as switch tube. The tunable pulse-forming network is resistor charged and an electronic shunt regulator servo maintains the PFN voltage within ± 0.15% of the set value. Detailed tests performed prior to installation and the successful operation itself show that a microwave system of this type is perfectly adequate for the separator under consideration, and is likely to remain usable at ultra high energies.

V. COUNTERS

During normal operating conditions, the beam performance is monitored in several ways. The intensity of the protons striking the target is measured from the voltage pulse across a 50 Ω resistor which is connected between target and ground. To achieve correct readings, a positive bias of 1 kV must be applied to the target. Much information can be gained from the beam profiles at the beam stopper and a vertically as well as a horizontally traversing finger counter is installed there. A paddle counter is also located at the stopper for normalization purposes. A fixed counter at the magnetic slit detects all beam-like particles entering the bubble chamber. The counters mentioned so far are all of the plastic scintillator type and their physical dimensions are given in Table V. The threshold gas Cerenkov counter from the old HESB No. 3 is placed ahead of the bubble chamber and serves as a qualitative but instantaneous monitor of the beam purity. However, considerable operational difficulties have to be faced with this counter.

Since the particles arrive in short bunches, about 10 nsec long, it is mandatory to integrate the photomultiplier outputs. The integrated signal is converted into digital form and transmitted to the control station for display on scalers. The magnetic slit counter is calibrated against the bubble chamber and the reading is directly in number of particles. The linear range of the electronic system is 10^3 and change of decade is possible by inserting a neutral density filter before the photomultiplier tubes.

VI. PERFORMANCE

The experience gained during several runs of the rf beam separator has showed that the design specifications were rather conservative and only minor adjustments have been necessary. The original set of klystrons is still in use, promising a long lifetime. Problems with the reliability of the high voltage regulators in the modulators were encountered, but improvements are possible without great effort. Slow phase drifts in the high power system require phase adjustments of 5 to 10° in the course of one day. Arcing of the deflectors when operated at a 12 MW level occurs at a rate of one arc per several hours. Accumulated effects during conditioning of the deflectors have caused the failure of both deflector windows, however the klystron windows remained intact.

The number of transmitted W particles and the purity of the beam is determined by an intricate interplay of source slit setting, beam stopper size, imparted deflections, beam acceptance, and particle yield. It was found necessary, therefore, to determine anew for each experiment the optimum working conditions. The case of 12.8 GeV/c K^- beams may serve as an example. The magnet tuning is performed with particles of positive polarity. The section up to the first deflector is tuned by using a slow spill of protons

which are diffraction scattered from an internal target. The high background within the AGS shielding is overcome by searching for the shadow of the target with counters in coincidence. The tuning of the subsequent sections uses then a fast ejected beam and integrating counters. After alignment of the beam optics, the tuning of the rf separator proper can start. The source slit is reduced to about 5 mm and deflection tests are run for each deflector (Fig. 3). Equality in deflection can be accomplished to within a few percent. With both deflectors on, the rf phase is adjusted until the deflections of U particles, i.e., p and π in the case considered, cancel exactly. It is possible at this point to detect a net deviation from the nominal momentum, if cancellation for p and π occur at different phase settings. A 1% error in momentum is in this way easily detected and corrected for. This check on the momentum can only be performed with positive polarity beams because of the required fluxes of the particles involved. The beam is now switched to negative polarity and the separator tuning is repeated. Optimum conditions are achieved as follows: The total deflection is made 2 mrad peak for W particles having traversed both deflectors. The beam stopper is set to about 4 cm, which corresponds to 2.7 mrad in the deflector. The source slit is then opened to a value which yields on the average 8 to 10 tracks in the bubble chamber (Fig. 4). The presence of K mesons in the purified beam is verified with the Cerenkov counter. An indirect, yet quite reliable, indication for the presence of W particles in the beam is obtained by comparing the magnetically scanned horizontal images at the magnetic slit with both deflectors turned on and then off (Fig. 5). Most directly the purity of the beam can be ascertained by scanning of the pictures for τ decays in the chamber. Preliminary

scanning results indicate a purity of at least 85% for the 12.8 GeV/c K^- run. While running, correct operation of the rf separator is monitored by the vertical finger counter which is set at the edge of the cancelled image of the U particles and by the Cerenkov counter which is set below the kaon threshold.

ACKNOWLEDGEMENTS

For the redaction of this paper liberal use was made of publications, reports and private notes of colleagues at Brookhaven, Yale, and elsewhere, and the author would like to express his gratitude to all who provided him generously with the needed information. Thanks are due to Dr. J.P. Blewett for helpful comments on the manuscript. For a complete list of references on the subject discussed, the reader is referred to the available literature or to a forthcoming paper by H.W.J. Foelsche, H. Hahn, H.J. Halama and J. Sandweiss in the Review of Scientific Instruments.

TABLE I. Runs performed with the rf beam separator as per 1 September 1966.

Type	Momentum (GeV/c)	Pictures
K^-p	12.8	187 000
	9.1	58 000
	7.4	49 000
K^+p	12.8	79 000
	7.4	59 000
K^-d	12.8	86 000

TABLE II. Parameters of rf beam separator at Brookhaven.

Total length	129 m
Deflector distance	40 m
Design wavelength	10.5 cm
Design momentum (K π)	9.245 GeV/c
Length of	
- Pre-momentum analysis section	33 m
- Separation stage	69 m
- Post-momentum analysis	27 m
Vertical focal length of	
- Recombination section	22.6 m
- Stopper section	14.8 m
Vertical magnification	
- From mass slit to beam stopper	0.655
Stopper length (brass)	91 cm
Target (Be)	0.5 X 0.5 X 25 cm^3
Production angle	0^o
Intrinsic deflector acceptance	100 cm^2 μsterad
Solid angle accepted at target	7 μsterad
Momentum bite of	
- Pre-analysis	1%
- Post-analysis	$\approx$ 1%
Vertical angular divergence of beam at deflector	$\leq$ 0.8 mrad
Beam stopper size	$\approx$ 4 cm (2.7 mrad)
Peak deflection	
- Per deflector	ϵ_W^{-1} mrad
- After two deflectors	2 mrad
Loss in beam stopper	50 to 80%

TABLE III. Operating momenta and deflection efficiencies of K beams.

m	p (GeV/c)	On momentum				1% off momentum			
		ϵ_K	ϵ_U	ϵ_d	ϵ_d'	ϵ_K	ϵ_U	ϵ_d	ϵ_d'
1	12.81	0.730	0	0.196	0.165	0.740	0.063	0.432	0.372
2	9.05	0.998	0	0.406	0.180	0.995	0.126	0.810	0.358
3	7.39	0.633	0	0.576	0.017	0.595	0.188	0.980	0.030

TABLE IV. Deflector parameters.

Design wavelength	λ_o	=	10.495 cm
Operating frequency (v_p = c)	f	=	2856.17 MHz
Beam hole	2a	=	4.813 cm
Outer diameter	2b	=	11.671 cm
Period	h	=	2.624 cm
Slot width	d	=	2.098 cm
Phase shift per cell	φ	=	$\pi/2$
Phase error per cell	$\Delta\varphi$	=	2.7^{o} rms
Electrical length	ℓ	$\approx$	3.10 m
Group velocity	v_g	=	- 0.0204 c
Attenuation parameter	$\alpha\ell$	=	0.513
Filling time	t_f	$\approx$	0.5 μsec
Deflector constant	$K\ell$	=	5.22 $k\Omega^{\frac{1}{2}}$
Quality factor	Q	=	8800
Interaction parameter	R/Q	=	1.57 kΩ/m
Shunt impedance	R	=	13.8 MΩ/m

TABLE V. Physical dimensions of counters.

	Horiz. x vert. x beam
Finger counters at beam stopper	
- Vertically traversing	1 x 19 x 13 mm
- Horizontally traversing	3 x 38 x 13 mm
Paddle counter at beam stopper	152 x 152 x 13 mm
Magnetic slit counter	15 x 178 x 13 mm
Threshold gas Cerenkov counter	30 Ø x 213 cm

FIGURE CAPTIONS

Fig. 1 Schematic layout of rf separated beam ("beam 4") between AGS and 80" bubble chamber.

Fig. 2 Block diagram of microwave system for the rf beam separator.

Fig. 3 Vertical beam profile at beam stopper. Undeflected image is shown as solid line, deflected image due to one deflector is shown as dashed line.

Fig. 4 Typical vertical image widths of wanted and unwanted particles and beam stopper size in K beams.

Fig. 5 Horizontal profile at magnetic slit. Solid curve shows the condition with both deflectors on, dashed curve for both deflectors off.

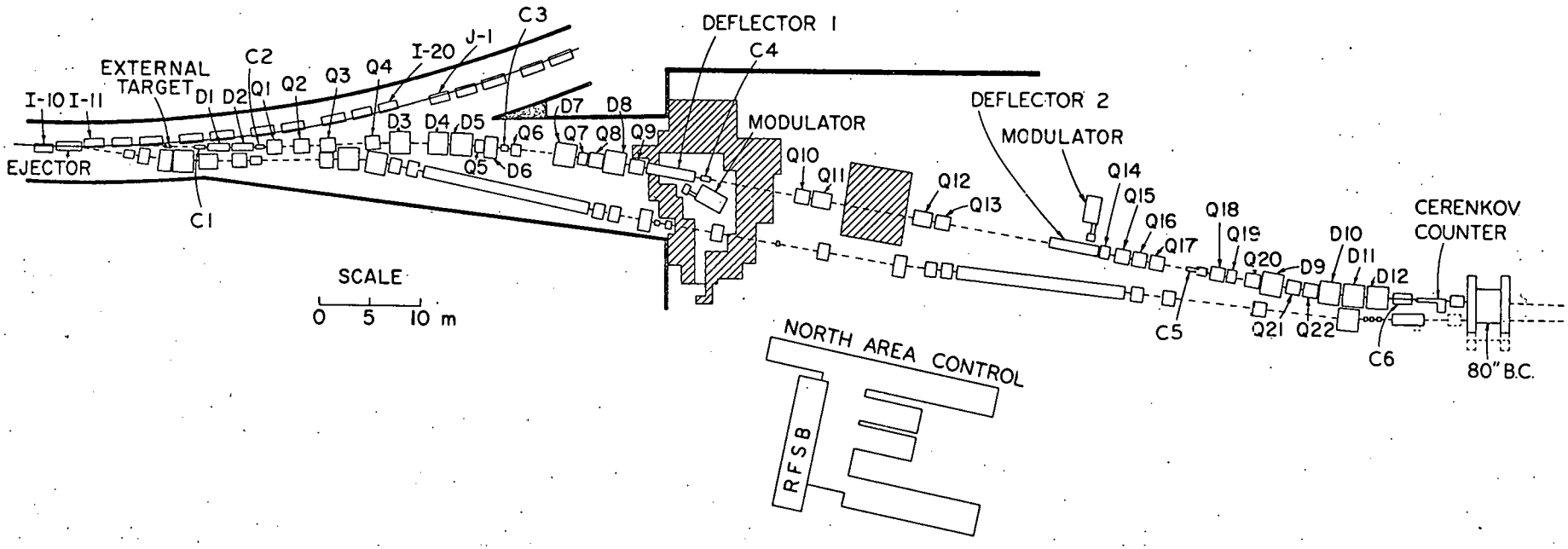
C3
DEFLECTOR 1
C4
J-1
I-20
C2
EXTERNAL
TARGET
Q4
Q3
Q2
Q1
DI
D2
I-10
I-11
D3
D4
D5
D7
D8
Q6
Q7
Q8
Q9
MODULATOR
DEFLECTOR 2
MODULATOR
EJECTOR
Q5
D6
Q10
Q11
Q12
Q13
Q14
Q15
Q16
Q17
Q18
Q19
Q20
D9
D10
D11
D12
CERENKOV
COUNTER
C1
SCALE
0 5 10 m
C5
Q21
Q22
C6
80" B.C.
NORTH AREA CONTROL
RFSB

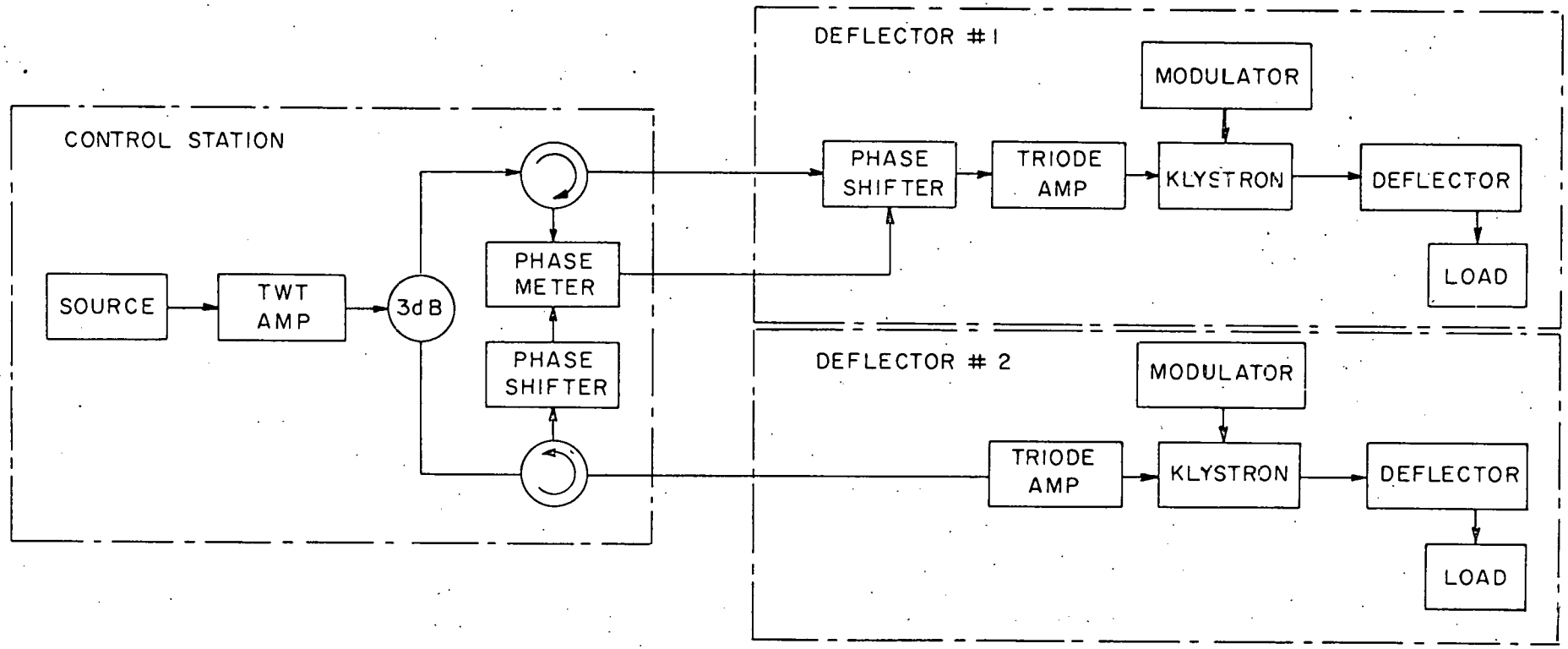
DEFLECTOR #1
MODULATOR
CONTROL STATION
PHASE SHIFTER
TRIODE AMP
KLYSTRON
DEFLECTOR
PHASE METER
LOAD
SOURCE
TWT AMP
3dB
DEFLECTOR # 2
MODULATOR
PHASE SHIFTER
TRIODE AMP
KLYSTRON
DEFLECTOR
LOAD

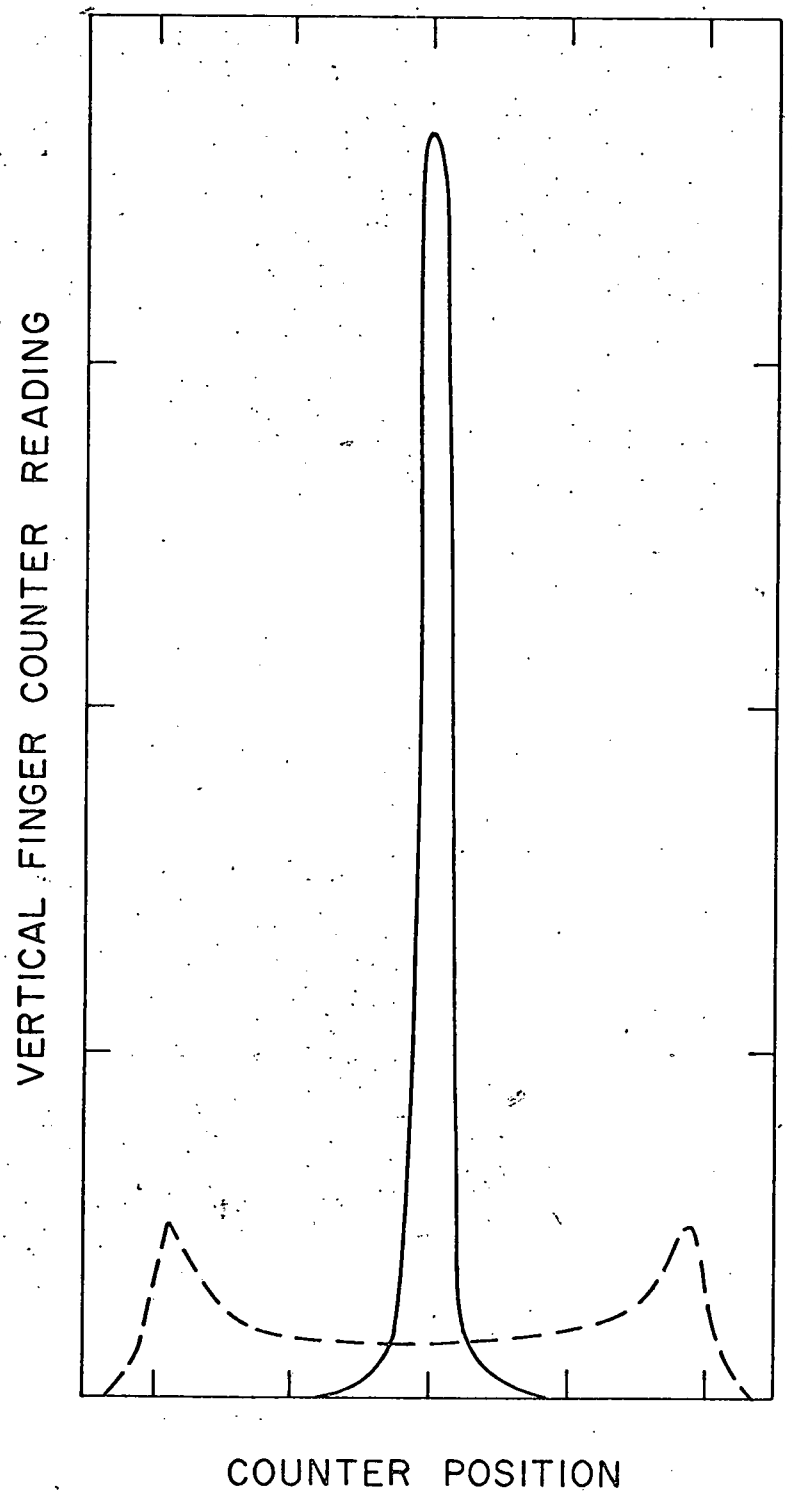

A photographic negative of this

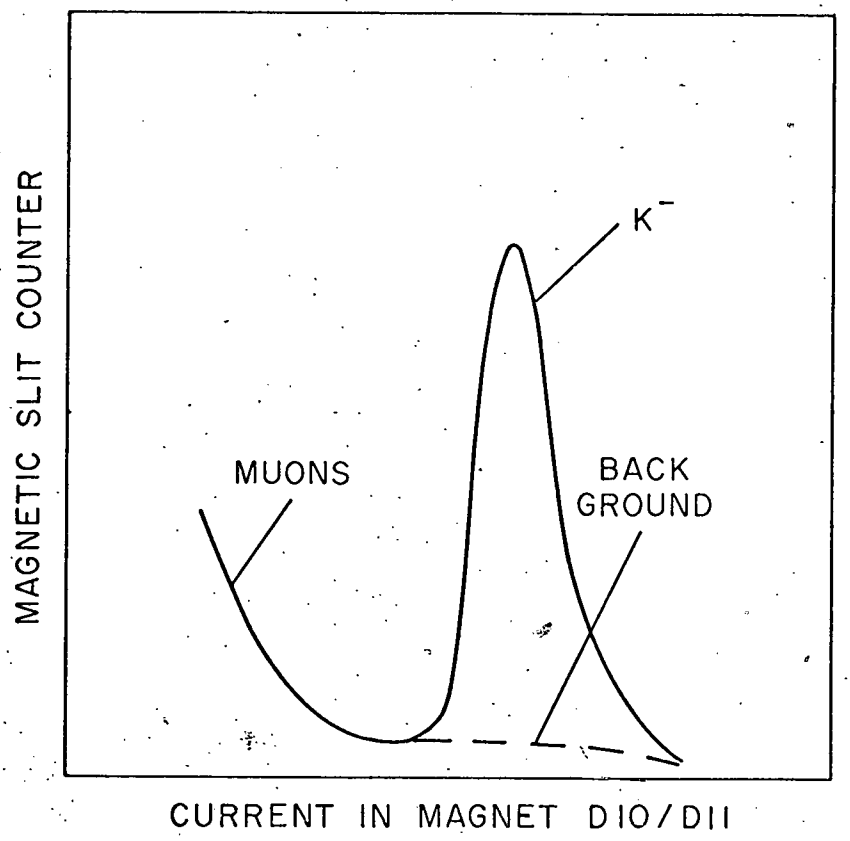
MAGNETIC SLIT COUNTER
K⁻
MUONS
BACK
GROUND
CURRENT IN MAGNET D10/D11